CEE 6200 Final Project Report
Cornell University
Instructor: Dr. Patrick Reed

Introduction to Rhodium and Multi-objective Robust Decision Making for Ecosystem Management

N. Blahut, A. Gangadhar, R. Maksimovic

Abstract: This report will focus on a hypothetical lake management problem to demonstrate how the Rhodium library can be used to facilitate multi-objective robust decision making to control phosphorus emissions into the lake and prevent eutrophication. The authors of the Rhodium library formulated the lake management problem in Rhodium to identify the Pareto optimal set of intertemporal management strategies. We used that formulation to replicate and analyze their results. We also used code available in the Rhodium library to perform a direct policy search for lake management strategies, and compared those results to the intertemporal solutions.

Keywords: Multiobjective robust decision making (MORDM); Rhodium; ecosystem management; visual analytics; sensitivity analysis; eutrophication

1 Introduction

1.1 Phosphorus Pollution

Across the globe, physical and biological systems are undergoing shifts in regional temperatures, leading to increased uncertainty in our understanding of these systems (Parry et al. [2007]). A few things are becoming increasingly apparent though. With an increase in urban land cover and also in the use of fertilizers in agriculture, management of phosphorus in lakes is becoming more and more challenging. A lake with phosphorus input has two main states — oligotrophic and eutrophic. An oligotrophic lake is one with low nutrient inputs, low to moderate levels of plant cover, reasonably clear water and relatively high value of ecosystem services. Eutrophic lakes on the other hand have high nutrient inputs, high plant production, turbid water, anoxia, toxicity and diminished value of ecosystem services. Thus eutrophication negatively impacts the health of a lake ecosystem, and reduces the net value derived from the lake (Postel and Carpenter [1997]). Here nutrients refer to mainly nitrogen (N) and phosphorus (P) inputs that are by-products of agriculture, forestry and urban development. Eutrophication is ultimately caused by an excessive input of these nutrients into a lake.

1.2 The Shallow Lake Problem

The focus of this report is a hypothetical problem about a town that must decide how much phosphorus to release annually into a shallow lake. As discussed in the previous section, the activities that lead to excessive phosphorus inputs in lakes, such as urban development and agriculture, are those that generate economic revenues, but the value of the lake ecosystem declines when there is a high phosphorous concentration in the lake. Since the lake is shallow, if the lake enters a eutrophic state, it will not naturally recover (Carpenter et al. [1999]), and this will lower the profits the town can earn from the lake ecosystem. That said, there is a clear trade-off between the maximum allowable

annual phosphorus input into the lake and the economic utility, which makes the shallow lake problem, or simply the lake problem, an interesting study in the effects of ecosystem dynamics on economic analysis (Carpenter et al. [1999], Quinn et al. [2017]).

The advantages of choosing the lake problem as the focus of our report include: (1) the trade off between ecological health and economic utility in the lake problem is analogous to several other environmental issues, (2) the model is relatively simple to derive since the rate of eutrophication is obtained from a straightforward mass balance, (3) the lake problem accounts for stochasticity, irreversibility, uncertainty, and (4) the lake problem is well-documented and modelled in literature, providing us with multiple references for our results (Carpenter et al. [1999]).

1.3 Multiobjective Robust Decision Making

The hypothetical lake problem under consideration exemplifies three difficulties that are common in ecosystem management: "(1) the presence of several stakeholders with conflicting objectives (2) the potential for highly nonlinear threshold responses, and (3) the underlying deep uncertainties" (Singh et al. [2015]). In the context of the lake problem, competing stakeholders could include environmentalist groups and phosphorus generating industries. The potential for highly nonlinear threshold responses is represented by the shallow lake's inability to recover after it passes a certain concentration of phosphorus. Lastly, there are underlying deep uncertainties regarding the natural phosphorus inflows to the lake, lake characteristics, and the time value of money.

Multi-objective robust decision making is a useful approach to manage complexities associated with ecosystem management, which are described in the former paragraph. In four steps, the MORDM process goes as follows:

1. Initial problem formulation.
2. Multi-objective evolutionary algorithm to find the Pareto approximate set of solutions.
3. Uncertainty analysis.
4. Subject candidate solutions to a scenario discovery process (Kasprzyk et al. [2013]).

Visual analytics are an important part of the MORDM process, and are utilized throughout. For example, visual analytics are employed to evaluate the collection of candidate policies that are generated through optimization and illustrate whether or not a candidate solution is robust to a wide array of possible future conditions.

1.4 The Rhodium Framework

The Rhodium Framework is an open source Python library, which contains all the data structures and classes that are required to perform the MORDM analysis described in the previous section (Hadjimichael et al. [2015]). The Rhodium GitHub repository also includes a Python notebook, which implements the Rhodium library to model the lake problem, generate intertemporal management policies, produce visual analytics, and perform a sensitivity analysis on said policies. From this point forward, this notebook will be referred to as the Lake Problem Notebook. The Rhodium library also includes code, which can be used to alter the Lake Problem Notebook search strategy, so that it returns parameterized policies.

2 Modelling and Optimization of the Lake Problem

2.1 Lake Problem Objectives

The Lake Problem Notebook defines mathematical relationships between parameters with well characterized uncertainty (phosphorus removal rate, phosphorus recycling rate, mean of natural inflows, standard deviation of natural inflows, and utility discount factors a annual pollution limits) and the decision variable (policy for limit on annual phosphorus input) and objective values of interest (maximum P concentration in the lake, utility, reliability, and inertia). Those mathematical relationships are described in the following paragraphs.

Minimize maximum phosphorus limit. The dynamics of P recycling in the lake are modeled using the theoretical model of lake nutrient dynamics developed in Carpenter et al. (1999). In this model the water quality can transition between oligotrophic and eutrophic equilibrium. The parameters in this model are also derived from Carpenter et al. (1999) which the authors used to abstract the P dynamics in Lake Mendota, Wisconsin (Quinn et al. [2017]).

$$X_{t+1} = X_t + a_t + Y_t + \frac{X_t^q}{1 + X_t^q} - bX_t \tag{1}$$

In Equation 1, X is the concentration of P in the lake normalized with respect to the P value at which recycling reaches half the maximum rate, a represents the controlled point source P inputs, Y are the uncontrolled non-point source P inputs modeled with a log-normal distribution having a mean μ and standard deviation σ, the parameter q is recycling rate of P in the lake, and b is the decay rate of P in the lake.

Maximize economic utility. For a system with N simulations over T years, the expected economic utility is calculated using the below equation.

$$U = \frac{1}{N} \sum_{i=1}^{N} \left(\sum_{t=0}^{T-1} \alpha a_{t,i} \delta^t \right) \tag{2}$$

In our study, $\alpha = 0.4$ and $\delta = 0.98$ (Ward et al. [2015]).

Maximize system reliability. The reliability of the system is measured as the average fraction of time the lake is below the threshold of irreversible eutrophication.

$$R = \frac{1}{NT} \sum_{i=1}^{N} \left(\sum_{t=1}^{T} \theta_{t,i} \right) where\, \theta_{t,i} = \begin{cases} 1, X_{t,i} < X^{crit} \\ 0, X_{t,i} \geq X^{crit} \end{cases} \tag{3}$$

Here X_{crit} is the critical P threshold beyond which irreversible eutrophication occurs. The reliability of the system is constrained to be equal to or above 75% in order to get optimal policies that are feasibly reliable, and not exceptionally likely to fail.

Maximize inertia of the optimal policy. Inertia of a policy refers to its stability, which in this case is desirable since a change in P limits would require large investments in tertiary treatment processes. This inertia can be calculates as follows.

$$I = \frac{1}{N}\sum_{i=1}^{N}\left(\frac{1}{T-1}\sum_{t=1}^{T-1}\varphi_{t,i}\right) where\ \varphi_{t,i} = \begin{cases} 1, a_{t-1,i} - a_{t,i} < I_{imit} \\ 0, \\ a_{t-1,i} - a_{t,i} \geq I_{limit} \end{cases} \quad (4)$$

I is the average fraction of T-1 time steps across the N simulations run, and I_{limit} is some limit that the reductions need to be less than. The latter value depends on the stakeholders' needs.

2.2 Open-loop Control via Intertemporal Optimization versus Closed Loop Control via Direct Policy Search

Similar to recent work by Quinn et al. (2017), we ran optimization trials for the shallow lake problem with two solution strategies: open-loop control via intertemporal optimization and closed loop control via direct policy search (DPS). In both cases, we used the Non-Selective Genetic Algorithm II(NSGAII) for a 100 year planning horizon. The Rhodium framework also supports other evolutionary algorithms; we used NSGAII because it is the simplest to implement.

The mathematical relationships described in the previous section are the same for the DPS and intertemporal control strategy searches. Intertemporal optimization looks for the optimal amount of P to release each year, based on the initial state of the model (Quinn et al. [2017]). Optimization with the DPS method works by parameterizing policies, simulating the parameterized policies, and then optimizing them (Quinn et al. [2017]). This process returns a collection of polices in the form of rules, which use the current state of the lake to determine the optimal amount of phosphorus to release in the upcoming year (Quinn et al. [2017]). The DPS strategy's incorporation of system feedback tends to produce policies that are more robust and adaptable. (Quinn et al. [2017]).

2.3 Results of Multiobjective Optimization

100 optimal policies were returned for the intertemporal optimization and DPS. We used Rhodium's built in visual analytics to analyze said policies. A comparison of the visual analytics produced for the policies returned by the DPS vs intertemporal optimization is included in the following section.

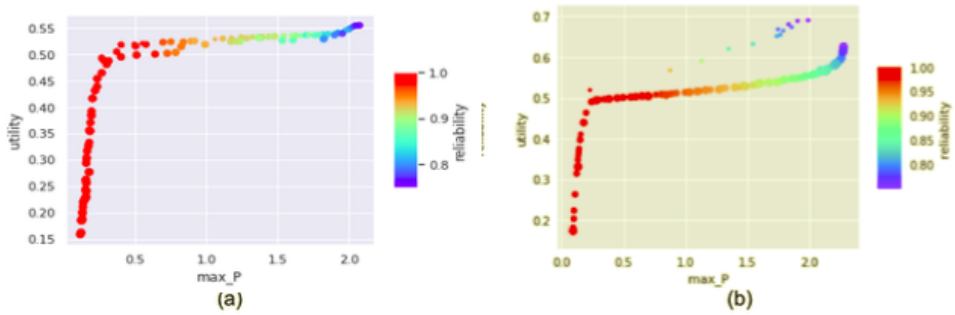

Figure 1. Scatter plot showing the Pareto front of the lake problem optimized using the (a) intertemporal and (b) direct policy search (DPS) method. The x-axis shows maximum allowed P emissions, the y-axis shows the utility objective. The color of the markers represent the reliability while the size of the marker (small to big) corresponds to (increasing) inertia.

Figure 1 shows that the intertemporal optimization and DPS returned policies with similar Pareto fronts. The main difference is that the utility of high max P generating DPS policies was slightly higher than policies generated by intertemporal optimization.

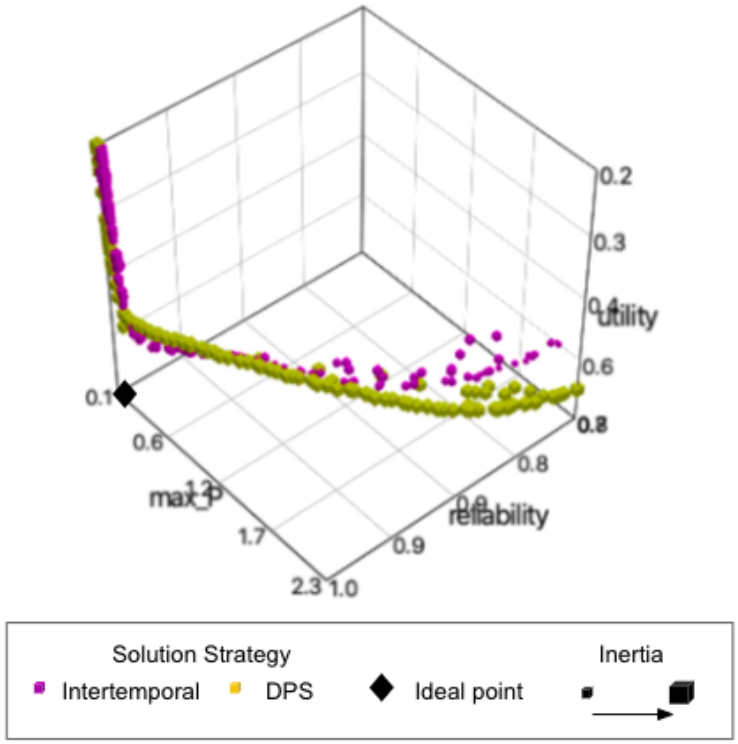

Figure 2. 3D scatter plot showing the Pareto front of both the intertemporal (pink) and DPS (yellow) methods. The optimal point is represents by the black diamond. The x-axis shows the max P limit, the y-axis shows the economic utility, the z-axis shows the reliability and the size of the marker indicates the inertia of the policy.

The 3D scatter plot of the approximate Pareto front for the intertemporal and DPS solution strategies shown in Figure 2 again illustrate that the fronts are very similar, but the DPS strategies tend to be slightly closer to the ideal point.

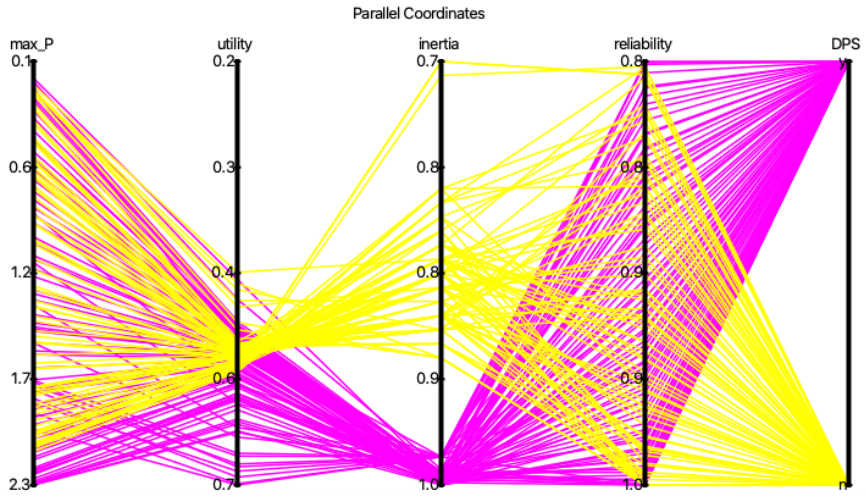

Figure 3. Parallel axis plot showing all optimal policies for intertemporal (yellow) and DPS method (pink), plotted against normalized axes showing all four objectives. Note that the colors are switched from the previous figure

The parallel axis plot in Figure 3 represents the optimal policies generated by the intertemporal (yellow) and DPS (pink) methods. These visuals make it clear that DPS polices are generally have much higher inertia values than their intertemporal counterparts.

Figures 10 and 11 (included in the appendix) show the matrices of pairwise comparison of objectives for solutions generated by the DPS and intertemporal optimization show very similar trade offs between objective performance for the generated polices in the baseline state of the world.

2.4 Evaluation of Policy Robustness with Rhodium

Next, we used Rhodium to see how the solution sets generated by DPS and intertemporal optimization, which performed similarly in our baseline case of the world, fared under deep uncertainty. We selected two pairs of policies to compare with Rhodium's sensitivity analysis tools: (1) the profit-maximizing intertemporal and DPS policies (2) the intertemporal and DPS solutions that performed the most similarly across all objectives in the baseline state of the world. The parallel axis plot in figure 4 shows how the pair of "comparable" solutions, generated by either DPS or intertemporal optimization, performed in the baseline state of the world.

The procedure for evaluating candidate policies in multiple states of the world for the lake problem is well-documented in the Lake Problem Notebook, and is the basis of our uncertainty analysis. To create a "state of the world" we defined uniform distributions for our uncertain parameters which include the lake's recycling exponent, decay rate, mean and standard deviation of natural P inflows, and future utility discount rate, and then take a random sample of each parameter. The range of each parameter is listed below:

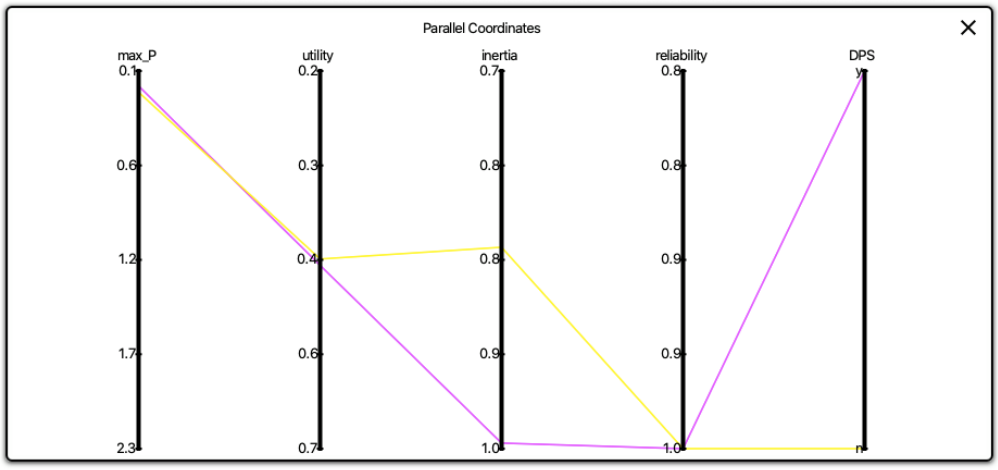

Figure 4. Parallel axis plot, which represents the comparable DPS (pink) and intertemporal (yellow) policies' objective values in the baseline state of the world

$$decay\ rate = unif(.1, .45) \tag{5}$$

$$recycling\ exponent = unif(2.0, 4.5) \tag{6}$$

$$mean\ of\ natural\ inflows = unif(.01, .05) \tag{7}$$

$$standard\ deviation\ of\ natural\ inflows = unif(.001, .005) \tag{8}$$

$$future\ utility\ discount\ rate = (.93, .99) \tag{9}$$

The combination of those selected parameters represents a state of the world (SOW). For our analysis, we created 1000 possible SOWs.

Once multiple possible states of the world were created, we returned to the original lake problem model and input our various states of the world along with our aforementioned policies of interest. Then, we ran the model to see what objective values the selected policies returned in the multiple states of the world we generated.

3 Sensitivity Analysis

3.1 Methods

In order to perform sensitivity analysis, we explored a number of different methods. The Patient Rule Induction Method (PRIM), Classification and Regression Trees (CART), Sobol Sensitivity Analysis, and One at a Time (OAT) Sensitivity Analysis. These functions allowed us to explore how policies would perform in different States of the World (SOWs).

PRIM is a bump-hunting algorithm that seeks to trade-off between density and coverage of a region. Coverage is the percent of the overall area contained in the higher density bump, and density is the percent of correctly identified points in the high density region. In order to identify regions, PRIM starts with an entirely unconstrained region shaves away the edge that will maximize density most efficiently. The algorithm does not suggest an

optimal trade-off between coverage and density but rather allows the user to visualize the relationship (Bryant and Lempert [2010]).

CART is another method of visualizing the trade-offs in data. It produces a tree where results are classified as meeting the given criteria or not with increasing accuracy. Gini indices represent the fraction of the sample that is misclassified at a particular node, and the algorithm seeks to minimize Gini indices within the bounds of the parameter for the minimum samples in each leaf of the tree. Lowering the minimum samples per leaf threshold can increase accuracy at the expense of potentially overfitting to the data.

Sobol Sensitivity Analysis is a global sensitivity analysis method. It provides information about which parameters drive the sensitivity of the model overall rather than at a specific point. The algorithm explores how much of the total variance is driven by a given parameter. The first order sensitivity for a parameter i is

$$S_i = \frac{V_i}{V} \tag{10}$$

and total order sensitivity is given by

$$S_{T_i} = 1 - \frac{V_{\sim i}}{V} \tag{11}$$

where V is the total variance. The total order variance makes it possible to explore how interactions between parameters drive uncertainty.

OAT Sensitivity analysis is centered around the point of interest, and explores how changes in parameters around the specified point impact the system. This information is less general than the Sobol Sensitivity Analysis, but provides information about which parameters will have the biggest impact on the solution being considered. OAT sensitivity analysis is conducted by varying only one parameter at a time, and relies on the assumption that parameters are independent.

3.2 Results and Observations

Comparing the trade-offs between coverage and density for the utility maximizing intertemporal and DPS results in Figure 5 shows that the intertemporal result needed four restrictions to create a region of density 1.0 while the DPS result only needed two restrictions. Interestingly, the number of restrictions does not have a strong impact on the coverage, and both Density vs. Coverage plots have a similar shape where the relationship where the density benefits of restricting coverage are decreasing. The region of density 1 found by PRIM in the intertemporal result has 50.9% coverage, while for the DPS result the 52.1% coverage.

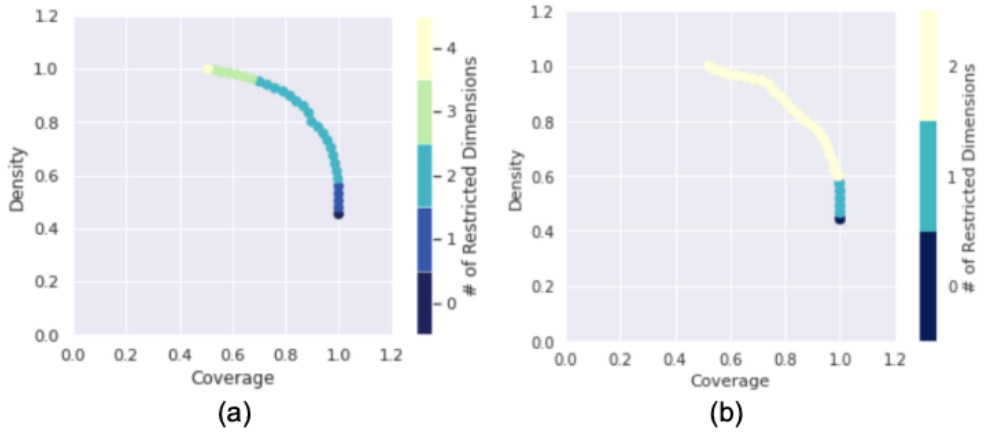

Figure 5. PRIM demonstrating the trade-off between density and coverage for (a) the utility maximizing intertemporal policy result, and (b) the utility maximizing DPS result.

The reason for this small change in coverage as compared to the number of restrictions can be seen in the projections shown in Figure 6. While the intertemporal result has four restrictions and therefore more projections, it can be seen that the restrictions on mean and standard deviation do not significantly reduce the coverage. The restrictions on b, the decay rate of Phosphorus, and q, the recycling rate of Phosphorus, have the most impact on coverage for both the intertemporal result and the DPS result.

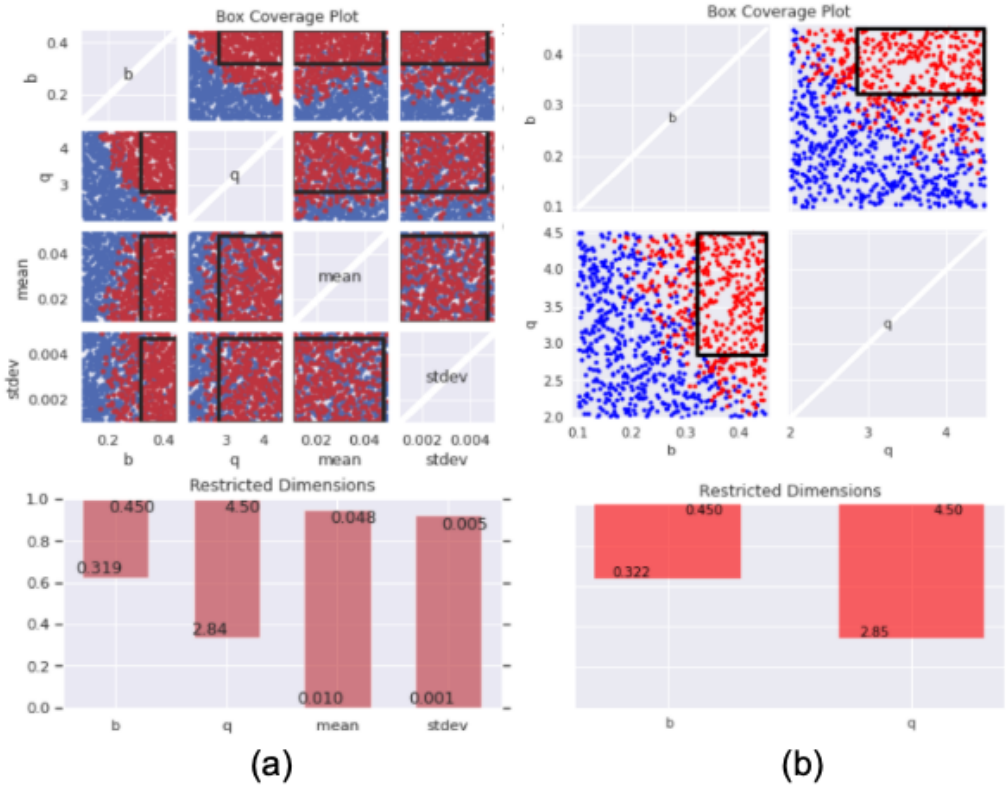

Figure 6. PRIM detail for the result with 100% density for (a) the utility maximizing intertemporal policy result, and (b) the utility maximizing DPS result.

Comparing the radial plots of the global sensitivities for the utility maximizing intertemporal and DPS plots in Figure 7 shows that the DPS result has many more second order interactions, but that the first order indices are relatively comparable. In both, b has the highest first order and total order variance, but in the intertemporal result the interactions between b and the mean and standard deviation are not sufficiently large to meet the standard for representation on the plot. Because of the particularly high utility of the DPS result as compared to the intertemporal result, it is not surprising that there are a large number of second order uncertainties associated with sensitivities to changes in two parameters at once.

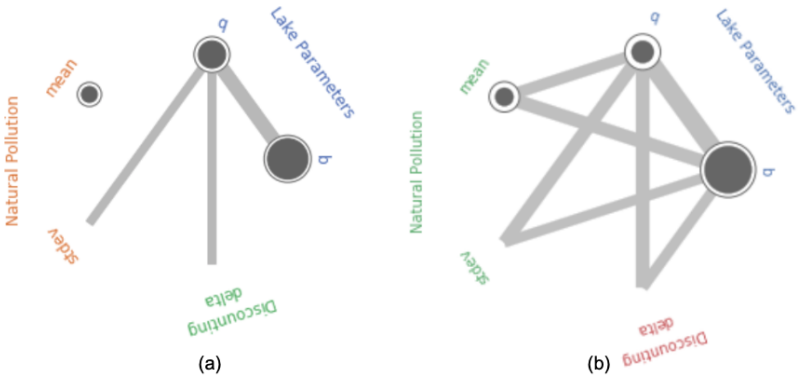

Figure 7. Radial plots showing the first, second, and total order indices for (a) the utility maximizing intertemporal policy result, and (b) the utility maximizing DPS result. Filled circles show first order indices, gray lines represent interactions, and empty circles show total order indices.

The uncertainties for the comparable policies shown in Figure 4 are shown in the bar graphs of Figure 8. For both the intertemporal policy result and the DPS result, the decay rate of Phosphorus is most significant globally, followed by the recycling rate of Phosphorus, and the mean of inflows. Because the plots are scaled equivalently, it can be seen that the magnitudes of these sensitivities are statistically equivalent.

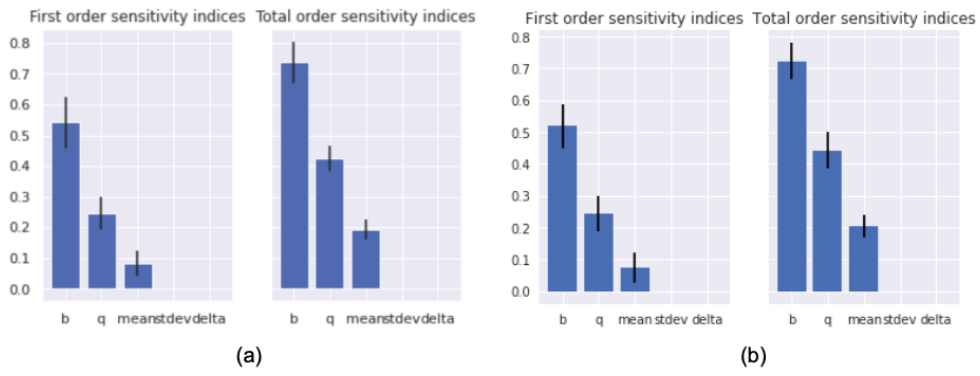

Figure 8. Bar plots showing the first and total order indices for the comparable (a) intertemporal policy result, and (b) DPS result.

In addition to the analysis of global sensitivities, the OAT sensitivities at the comparable policies in Figure 4 were considered. As shown in Figure 9, at those points for both the intertemporal policy result and the DPS result, b, the decay rate of Phosphorus comprised the largest percent of total variance, followed by the mean of inflows.

In addition to considering which variables drive total variance at the point of interest, the OAT sensitivity analysis provided an opportunity to visualize how changes in the inputs impacted reliability. For both the intertemporal policy result and the DPS result, an increased the decay rate of Phosphorus increases the reliability of the system. This is not surprising, since higher decay rates decrease the accumulation of phosphorus in the lake, thereby leading to lower phosphorus concentrations in the lake. In addition, in both cases increasing the mean of inflows is associated with a decrease in the reliability of the system. This result aligns with reason because if the concentration of phosphorus in the lake is high from natural inputs to begin with, the lake will be more sensitive to anthropogenic phosphorus inputs, and therefore more vulnerable to entering a eutrophic state. The plots also show that varying the future utility discount rate (d) does not impact the reliability of the system. This parameter impacts the utility objective more directly because it alters how utility in future periods is weighted.

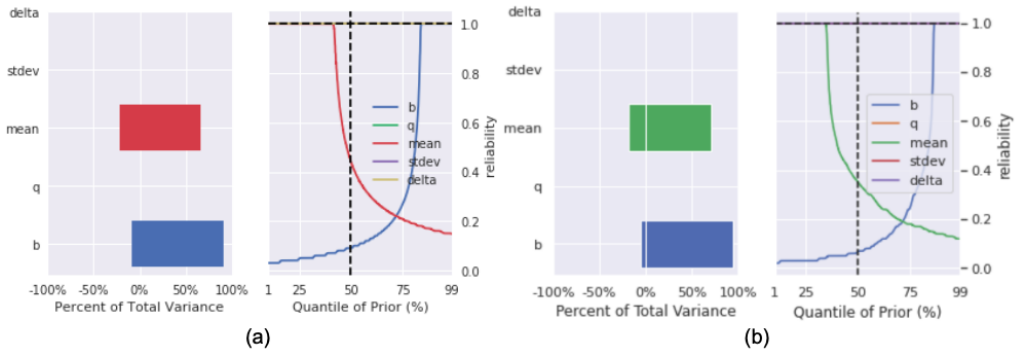

Figure 9. Plots showing the OAT Sensitivity Analysis for the comparable (a) intertemporal policy result, and (b) DPS result.

A classification and regression tree for the utility maximizing DPS result, Figure 12 in the appendix, shows that in the majority of SOWs the policy was unreliable, but that with only one dividing condition pertaining to the Phosphorus decay rate, over 70% of the sample could be correctly classified. Considering the conditions used to classify results as reliable or unreliable and their likelihoods allows for a more complete picture of whether a policy is likely to be robust enough to meet the needs of the community.

4 Conclusions

The Rhodium framework is a useful resource to generate and evaluate policies for ecosystem management problems. This report has shown how Rhodium can be used to carry out all the steps in the MORDM process and generate accompanying visual analytics. The evaluation of solutions generated via DPS and intertemporal optimization indicated that DPS solution strategies are generally more robust to uncertain future scenarios.

Although every "wicked problem" in policy planning is essentially unique, the Rhodium framework is flexible enough to mitigate many of the challenges associated with a wide variety of wicked problems (Rittel and Webber [1973]). For example, although there is on

immediate test to a solution to a wicked problem, evaluating a solution in multiple states of the world per the MORDM process, can provide useful insights to a solution's possible performance. Similarly, Rhodium's implementation of multi-objective evolutionary algorithms can narrow down wicked problems' innumerable set of possible solutions to focus on better ones. Cheers to Rhodium, and its contribution to making wicked problems considerably less wicked.

Acknowledgments

We as a team wanted to acknowledge that we felt this class handled the transition to virtual learning particularly well. Despite losing a week of class time and a homework assignment, we did not feel like the material was rushed and learned so many useful skills and techniques to address complex problems in and outside of water resources management. Thank you for the many office hours and extra help sessions that made this project possible. Again, we all learned a lot this semester and really enjoyed the course.

References

Bryant, B. P. and R. J. Lempert. Thinking inside the box: A participatory, computer-assisted approach to scenario discovery. *Technological Forecasting and Social Change*, 77(1):34 – 49, 2010.

Carpenter, S. R., D. Ludwig, and W. A. Brock. Management of eutrophication for lakes subject to potentially irreversible change. *Ecological Applications*, 9(3):751–771, 1999.

Hadjimichael, A., D. Gold, D. Hadka, and P. Reed. Python library for many-objective robust decision making and exploratory modeling. *Journal of Open Research Software*, 2015.

Kasprzyk, J. R., S. Nataraj, P. M. Reed, and R. J. Lempert. Many objective robust decision making for complex environmental systems undergoing change. *Environmental Modelling Software*, 42:55 – 71, 2013.

Parry, M., O. Canziani, J. Palutikof, P. van der Linden, and C. Hanson. *Climate Change 2007: Impacts, Adaptation and Vulnerability*. 01 2007.

Postel, S. and S. Carpenter. *Freshwater ecosystem services.* 1997.

Quinn, J. D., P. M. Reed, and K. Keller. Direct policy search for robust multi-objective management of deeply uncertain socio-ecological tipping points. *Environmental Modelling Software*, 92:125 – 141, 2017.

Rittel, H. and M. Webber. *Dilemmas in a General Theory of Planning*, volume 4, pages 155–169. 1973.

Singh, R., P. Reed, and K. Keller. Many-objective robust decision making for managing an ecosystem with a deeply uncertain threshold response. *ECOLOGY AND SOCIETY*, 20:12, 09 2015.

Ward, V. L., R. Singh, P. M. Reed, and K. Keller. Confronting tipping points: Can multi-objective evolutionary algorithms discover pollution control tradeoffs given environmental thresholds? *Environmental Modelling Software*, 73:27 – 43, 2015.

Appendix

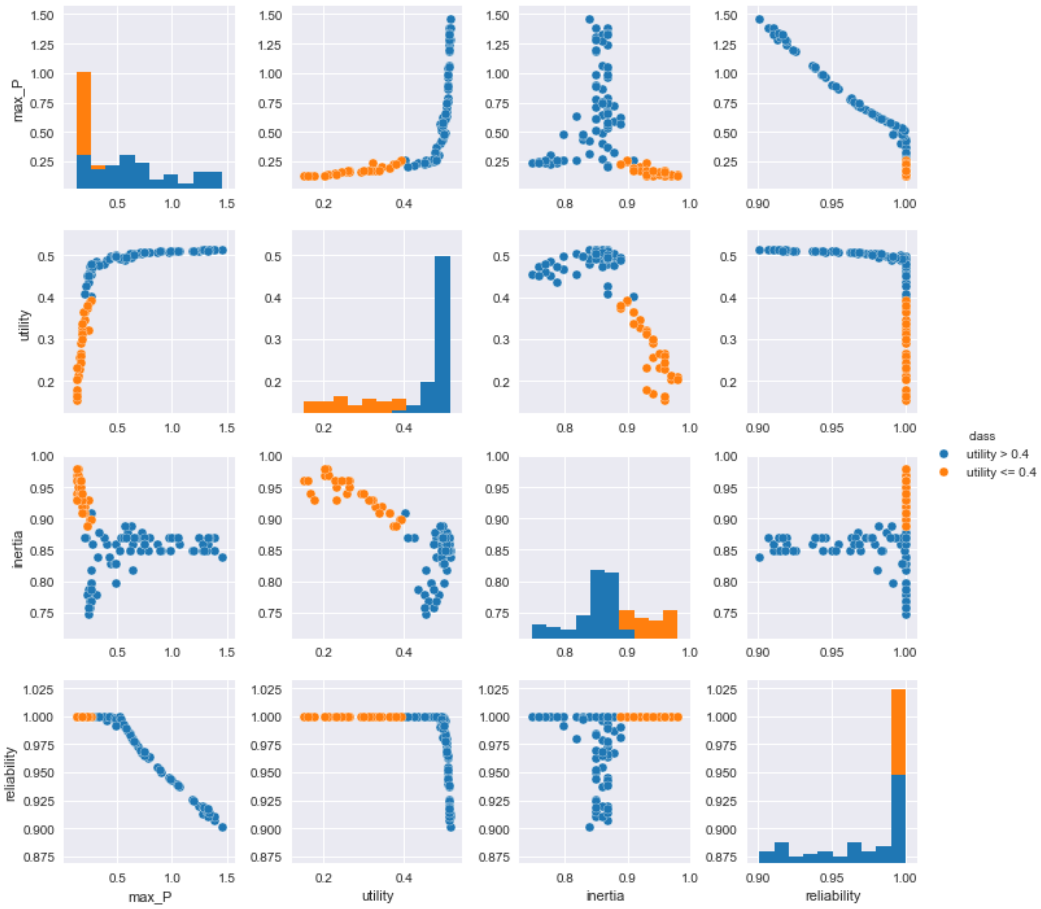

Figure 10. Scatter plot matrix showing pairwise comparison of all the objectives for the intertemporal policy search method. The brushing shows all points with utility greater than 0.4 as blue and the rest as orange. The histograms indicate the distribution of points along the x-axis for each objective.

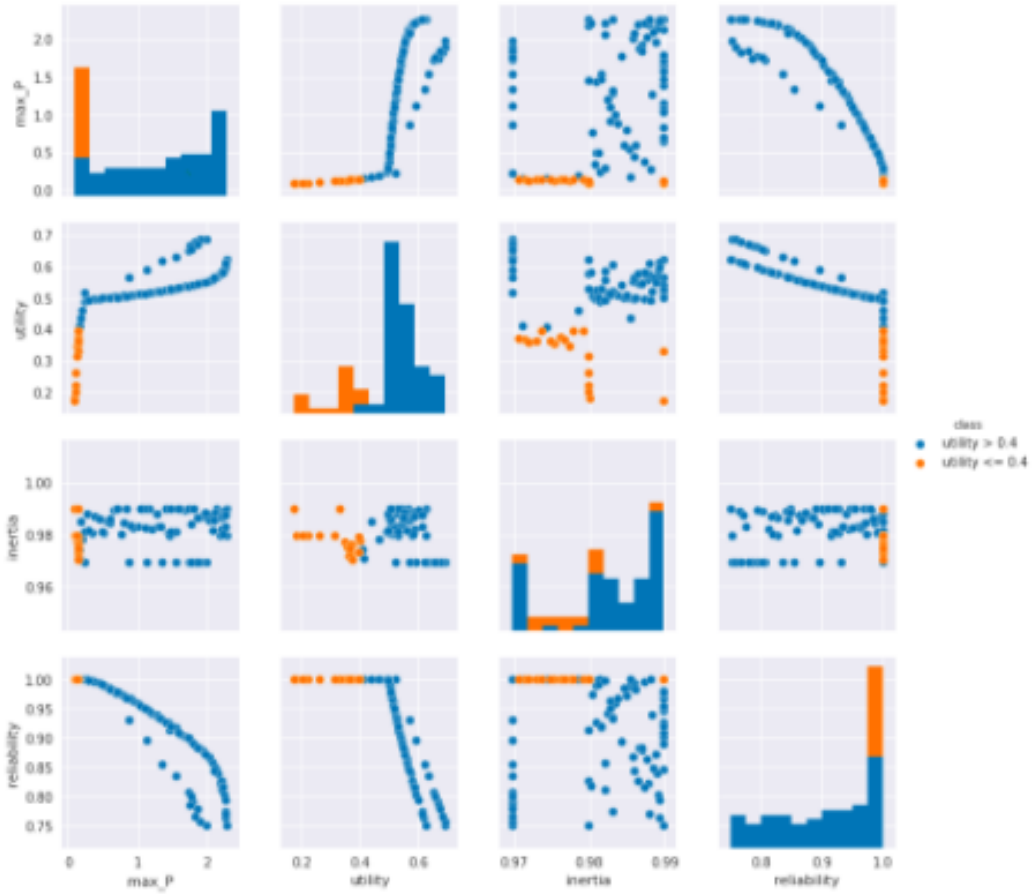

Figure 11. Scatter plot matrix showing pairwise comparison of all the objectives using the DPS method. The brushing shows all points with utility greater than 0.4 as blue and the rest as orange. The histograms indicate the distribution of points along the x-axis for each objective.

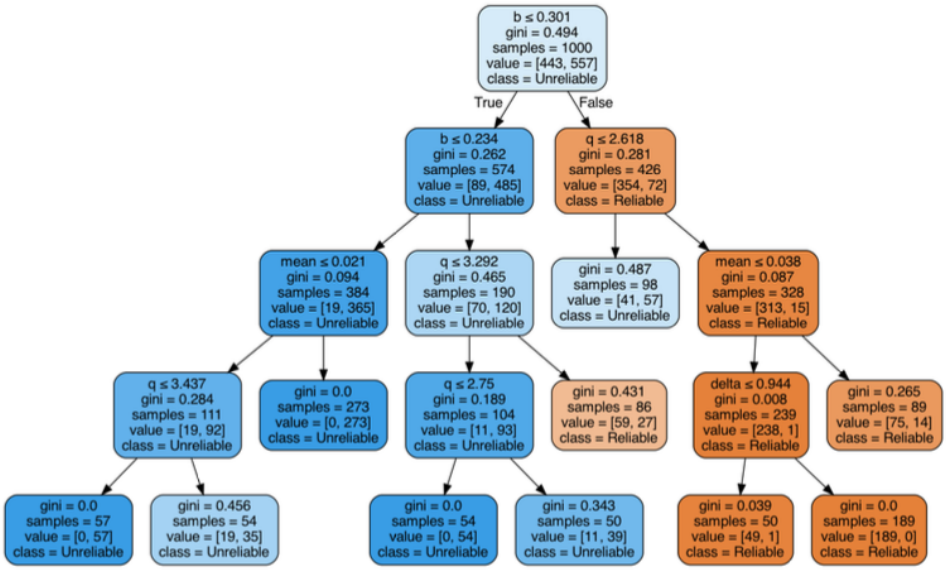

Figure 12. Classification and Regression Tree Classifying the utility maximizing DPS result as reliable or unreliable. Blue nodes are classified are unreliable, while red nodes are classified as reliable. The condition that used to separate nodes is listed at the top of each box, with the results satisfying that condition in the left child, and others in the right.